J. Am. Ceram. Soc., 94 [11] 3819–3824 (2011)
DOI: 10.1111/j.1551-2916.2011.04732.x

journal

Preparation of Dense and Porous Silicon Oxycarbide Submicrometer-Sized Spheres Using a Modified Stöber Process

Sandra Dirè, Valeria Tagliazucca,[§] Livio Salvadori, and Gian Domenico Sorarù[†]

Dipartimento di Ingegneria dei Materiali e Tecnologie Industriali, Università di Trento, Via Mesiano 77, 38123, Trento, Italy

Dense and highly porous silicon oxycarbide (Si–O–C) submicrometer-sized spheres, with diameters in the range 100–400 nm are synthesized through pyrolysis of sol–gel-derived hybrid precursors. A modified Stöber process is used for the synthesis of silsesquioxane submicrometer-sized particles from different organotriethoxysilanes RTES, $R = CH_3$, C_5H_{11}, and C_6H_5. The hybrid particles are transformed into dense inorganic Si–O–C submicrometer-sized spheres through a pyrolysis process in controlled atmosphere and the spherical morphology is kept provided that the glass transition temperature of the silsesquioxane network is higher than the onset of the polymer-to-ceramic transformation. The Si–O–C spheres are stable up to 1400°C. By HF etching the silica nanodomains present in the silicon oxycarbide structure, the dense Si–O–C particles can be further engineered and transformed into highly porous Si–O–C submicrometer-sized spheres with specific surface area up to 564 $m^2\ g^{-1}$ and pore volume up to 0.7 $cm^3\ g^{-1}$.

I. Introduction

Multicomponent Si–C–N–O ceramics obtained through pyrolysis of preceramic polymers, also known as Polymer Derived Ceramics (PDCs), have received increased attention in the last decades as structural and functional materials.[1] While initially PDCs were studied for their outstanding high temperature stability,[2] creep and crystallization resistance[3] and were proposed for processing fibers,[4,5] ceramic matrix composites[6] or for joining structural ceramics,[7] currently, the discovery of new functional features drives the research in this field. Indeed, intense luminescence with high external quantum efficiency has been reported for PDCs of the Si–O–C system, which make them excellent candidates for white LED applications.[8] Si–C–N PDCs showed anomalously high piezoresistivity[9] and Si–O–Cs displayed extremely high reversible capacity for lithium storage and are currently investigated to substitute the C anode in Li ion batteries.[10] It is believed that the remarkable properties of PDCs originate from their unusual nanostructure, which comprises mixed Si–C–N–O tetrahedra, silica/silicon carbide/silicon nitride nanodomains and graphene layers.[11,12]

One of the main disadvantages of PDCs is the difficulty in processing large and dense ceramic bodies. The high volumetric shrinkage, which occurs during the polymer pyrolysis, usually leads to differential strains, which ultimately result in the cracking of the component. There are two ways to overcome this problem: by reducing the shrinkage using fillers[13] or by decreasing the size of the ceramic sample. Accordingly, fibers and thin rods,[4,14] films,[8] and MEMS[15,16] can be successfully processed.

Currently, there is a great interest in studying the synthesis of spherical ceramic nanometric-sized particles to be used as reinforcing agent in nanocomposites, to reduce the sintering temperatures or, if they are porous, as drug-delivering media, catalyst support, filtrating/adsorbing media etc.[17–19] Many different oxide or mixed oxide systems have been already produced as spherical nanoparticles.[20–22] The Stöber process for the preparation of fine silica spherical particles is certainly one of the most well-known methods.[23] On the other hand, very few studies have been devoted to the preparation of fine SiC or Si–O–C particles although the PDC route should be ideally suited for the synthesis of these low-sized products. Fine silicon carbide particles have been prepared from polycarbosilane by precipitation processing,[24] Si–O–C spherical particles were obtained by emulsion processing from a commercial polysiloxane,[25] sub-micrometric capsules of silicon oxycarbide and silica have been obtained using a nanocasting route from polycarbomethylsilane and silica nanospheres[26] and finally, C/silica composite micro/nanospheres have been synthesized by aerosol-assisted spraying and pyrolysis from a phenolic resin/TEOS solution using sorbitan monooleate surfactant.[27] To the best of our knowledge, no study has been reported on the synthesis of spherical PDC Si–O–C nanoparticles from hybrid silica nanospheres obtained by a modified Stöber process. In principle, there are several advantages in using this approach: (i) the Stöber synthesis is a simple and well-known process that allows controlling the size of the nanoparticles, (ii) several different organoalkoxysilanes are commercially available and they can be co-hydrolyzed to vary the composition of the starting spheres, and (iii) doping the Si–O–C with extra cation such as B, Al, Ti, Zr can be easily achieved by adding to the starting solution the corresponding metal alkoxides. The interest for nanosized spherical silicon oxycarbide particles is manifold: besides the typical properties of ceramic materials, the Si–O–C particles bring, among others, new functionalities such as luminescence,[8] electrical conductivity,[28] or piezoresistivity.[29] In particular, nanometric-sized Si–O–C particles could be valuable as high capacity, high-charging rate anode materials for lithium ion batteries.[10] Moreover, based on the work of Wilson *et al.*[30] and on our previous experience on HF etching silicon oxycarbide glasses[31–33], the Si–O–C nanospheres could be further engineered to obtain highly porous Si–O–C-based nanoparticles, thereby expanding even more their potential application fields.

II. Experimental Procedure

Methyltriethoxysilane (MTES), phenyltriethoxysilane (PhTES), and amyltriethoxysilane (ATES) were purchased from ABCR (Karlsruhe, Germany) and Sigma-Aldrich (Steinheim, Germany). The chemical structures of organosilane precursors are shown in Fig. 1. Ethanol, hydrochloric

V. Sglavo—contributing editor

Manuscript No. 29425. Received March 11, 2011; approved June 06, 2011.
[§]Present address: Department of Heterogeneous Catalysis Max-Planck-Institut für Kohlenforschung Kaiser-Wilhelm-Platz 1 D-45470 Mülheim an der Ruhr Germany
[†]Author to whom correspondence should be addressed. e-mail: soraru@ing.unitn.it

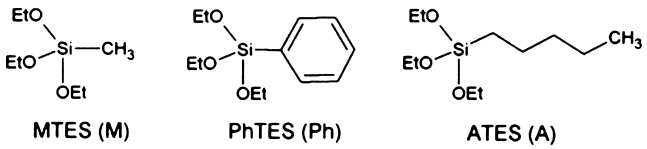

Fig. 1. Chemical structures of the organosilane precursors.

acid (37 wt%), and ammonia (30 wt%) were purchased from Sigma-Aldrich and used without any further purification.

(1) Stöber-Like Synthesis of Spherical Particles

The reactions were carried out in air at room temperature according to a published procedure.[34] The organotriethoxysilane, RTES, was dissolved in ethanol and reacted under stirring with the appropriate amount of HCl for 4 h (Step I). In the second hydrolysis–condensation step (Step II), an ammonia solution (2.3*M*) was added to the sol and the mixture was kept under stirring for 20 h ($EtOH:HCl:NH_3$ = 20:20:180, reagent/Si molar ratio). A white suspension was obtained and centrifuged at 5000 rpm for 15 min to separate the silica particles. The solid sample was collected, washed with distilled water three times and dried at 50°C for 24 h. The procedure was used for the synthesis of particles prepared with one or two different organotrialkoxysilanes ($R^{I}TES/R^{II}TES$) as shown in Table I.

(2) Particles Pyrolysis and HF Etching

The thermal treatments of the organosilsesquioxane spheres were performed using the furnace of a STA 409 Netzsch thermobalance, under flowing argon (100 cm^3 min^{-1}), in alumina crucibles. The samples were heated at 10°C min^{-1} up to 1000°C, 1200°C, and 1300°C and kept at the maximum temperature for 1 h. The etching process has been performed on particles pyrolyzed at 1300°C for 1 h with an aqueous HF solution (20 wt%). Particles were kept under stirring into the acid solution for 30 min, washed with distilled water, centrifuged at 6000 rpm for 5 min. The washing procedure was repeated three times.

(3) Physical and Structural Characterization

^{29}Si MAS NMR spectra were recorded with a Bruker 400 WB spectrometer (Bruker Instruments, Karlsruhe, Germany), equipped with a double band probe, at 79.50 MHz. Samples were packed in 4 mm zirconia rotors and spun at 6 kHz. ^{29}Si SP spectra were obtained with pulse length 4.3 μs, delay 5 s. Q^8M^8 was used as external secondary reference. Si units are labeled according to the usual NMR notation: Q, T, D, and X represent SiO_4, $SiCO_3$, SiC_2O_2, and SiC_4 units, respectively.

Thermal analyses (TG-DTA) were performed on a Netzsch STA 409 instrument (Netzsch-Gerätebau GmbH, Selb, Germany); the samples were heated in flowing argon (100 cm^3 min^{-1}) from 20°C up to 1500°C with a heating rate of 10°C min^{-1}.

Scanning electron microscopy was run using a FE-SEM Supra 40 Zeiss (Carl Zeiss NTS GmbH, Oberkochen, Germany) in high vacuum modality. The particle size distribution has been evaluated using the software ImageJ on images taken at 50.000× and counting at least 200 particles.[35]

N_2 sorption experiments were carried out at 77 K on an ASAP 2010 Micromeritics instrument (Micromeritics, Norcross, GA). The xerogel and pyrolyzed samples were degassed below 1.3 Pa at 25°C and 250°C, respectively. The specific surface area (SSA) was calculated by the BET equation in the interval $0.05 \leq p/p_0 \leq 0.33$ with a least-squares fit of 0.998. Single point total pore volume (TPV) was calculated at $p/p_0 = 0.995$. Pore size distribution was obtained from the adsorption branch using the BJH model.

XRD spectra were collected on a Rigaku DMax diffractometer (Rigaku, Tokyo, Japan) in the Bragg–Brentano configuration, using CuK_a radiation and a monochromator in the diffracted beam, in the range $2\theta = 10°–90°$ with a 0.05° step.

The chemical analyses were performed on selected pyrolyzed samples. O and C were measured and Si was estimated by difference to 100%. The elemental analysis was performed via hot-gas extraction using an O-analyzer (TC-436; Leco Instrumente GmbH, Mönchengladbach, Germany) and via combustion analysis with a C-analyzer (C-200; Leco Instrumente GmbH).

Table I. Compositions and Average Size of Silsesquioxane Nanoparticles (±SD)

Sample label	$R^{I}TES/R^{II}TES$	R^{II} mole (%)	Average size (nm)
M	MTES	–	170 ± 39
MA25	MTES/ATES	25	380 ± 78
MA50	MTES/ATES	50	175 ± 87
MA75	MTES/ATES	75	149 ± 60
Ph	PhTES	–	255 ± 62

III. Results and Discussion

(1) Morphological Characterization of Precursor and Pyrolyzed Particles

The Stöber-like approach, based on two-step hydrolysis–condensation process, employed for the synthesis of the organosilsesquioxane particles, is suitable for the production of submicrometer-sized regular spheres (Fig. 2), in agreement with our previous studies.[34,36] The nature of the organic group linked to silicon in trifunctional alkoxides affects nucleation and growth steps in solution, leading to particles with different diameter and size distribution (Fig. 2, Table I). The particle size distribution is always quite broad; nevertheless, it can be observed that the average diameter increases by changing from the methyl group (sample M) to the cumbersome phenyl group (sample Ph). For the mixed ATES/MTES samples, the largest particles are found for the MA25 composition, whereas for the pure MTES (sample M) or for samples with higher loads of MATES (MA50 and MA75), the diameter decreases.

Figure 2 also shows the effect of the pyrolysis process at 1000°C on the morphology of the silsesquioxane particles. FE-SEM micrographs highlight that M and MA25 samples retain their spherical shape after heating at 1000°C. By increasing ATES content in MA50 and MA75, a progressive aggregation of pristine particles is observed. In the case of Ph particles, no spheres are detected after pyrolysis at 1000°C and the sample consists of large fragments. It is well known that polymeric preceramic components can retain their shape during pyrolysis if they have been previously crosslinked, or, in case of thermoplastic silsesquioxane resins such as in the present study, if their glass transition temperature is higher than the starting decomposition temperature. In our laboratory, we have already shown that gel disks obtained from methyltriethoxysilane retain their shape after pyrolysis suggesting that the glass-transition temperature is, for this system, above the decomposition one.[37] On the other hand, it is known that particles prepared from phenyltriethoxysilane display a glass-transition temperature, T_g, at around 100°C and sinter at 10°C–50°C above T_g allowing to produce dense thick hybrid silsesquioxane coatings on various substrates.[38] Accordingly, the Ph submicrometer-sized particles can sinter well before the onset of the organic-to-inorganic transformation, thereby leading to the formation of large featureless fragments and prevents obtaining spherical Si–O–C particles from this precursor. Indeed, the micrograph reported in Fig. 2 of the Ph precursor pyrolyzed at 1000°C shows a large

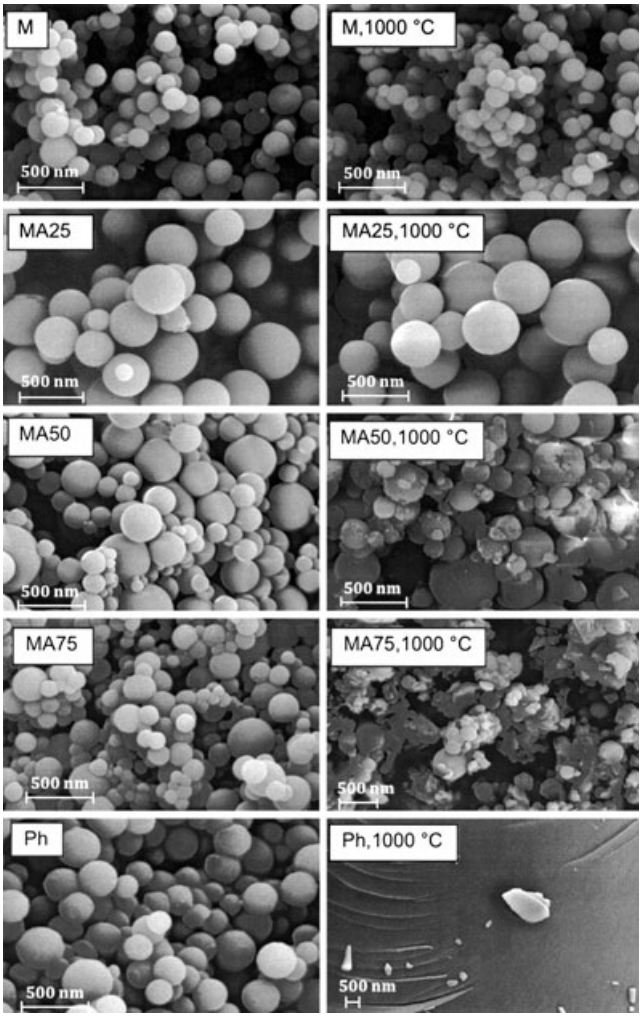

Fig. 2. FE-SEM micrographs of hybrid samples at the xerogel state and after pyrolysis in Ar at 1000°C.

fracture surface derived from a large Si–O–C piece. For the ATES/MTES systems, it seems conceivable to think that the presence of the long organic $–CH_2–CH_2–CH_2–CH_2–CH_3$ moieties acts as a plasticizer in the organic silsesquioxane network, thereby decreasing the glass-transition temperature. Accordingly, the shape of the particles after pyrolysis is retained only for the sample with the lowest ATES content, MA25, and it is progressively lost by increasing the ATES load, as for the MA50 and MA75 samples.

On the basis of these results, which showed that only the M and MA25 nanoparticles retain their shape after pyrolysis at 1000°C, we decided to focus our work on these two compositions.

(2) Pyrolysis Process and Structural Characterization of Si–O–C Submicrometer-Sized Spheres

Figure 3 reports the TG traces recorded in flowing Ar up to 1500°C for M and MA25 samples. The behavior of the M composition is in good agreement with our previous studies performed on micrometer-sized powders.[39] The total weight loss up to 1000°C due to the organic-to-inorganic transformation (Table II) is higher for MA25 (27%) than for M sample (13%). For M sample, the weight loss is concentrated between 700°C and 900°C, whereas for the MA25 composition before the 700–900 step, another decomposition process is active between around 400°C and 600°C. Based on the similarity of our silsesquioxanes systems with those already reported in the literature,[40–42] the thermogravimetrical analysis can be discussed as follows: The first mass-loss event of

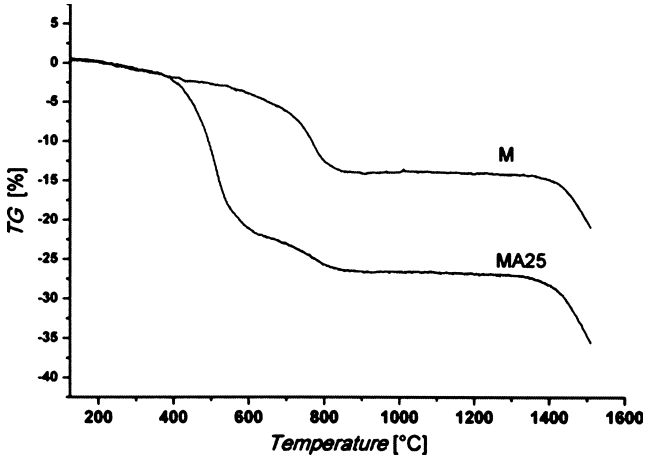

Fig. 3. TG traces of M and MA25 samples in Ar up to 1500°C.

Table II. Chemical Composition and Weight Loss for the Studied Si–O–C Particles Pyrolyzed at 1200°C for 1 h

Sample	C (wt%)	O (wt%)	Si (wt%) †	Weight loss (wt%) ‡
M	11.7	39.6	48.7	13
MA25	13.4	37.5	49.2	27

†Si has been evaluated as difference to 100%.
‡Measured from TG analyses in the range 20°C–1000°C.

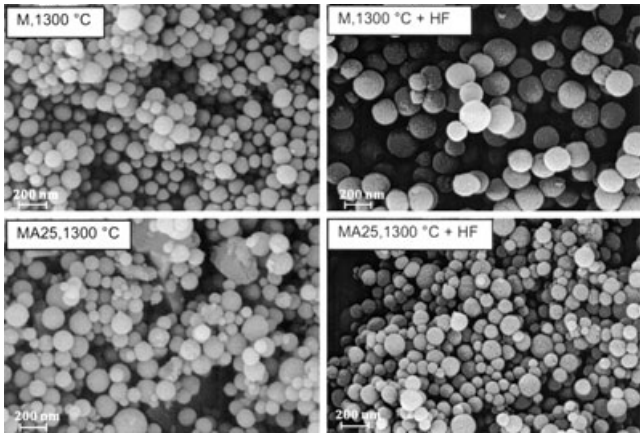

Fig. 4. FE-SEM micrographs of M and MA25 particles after pyrolysis in Ar at 1300°C for 1 h and subsequently HF etched.

the MA25 sample can be probably ascribed to the decomposition of the long aliphatic $–C_5H_{11}$ chain of ATES leading to the loss of carbon atoms not directly linked to the silicon atoms. Indeed, it has been already proposed that, for alkyl-modified silsesquioxane precursors to Si–O–C glasses, only the C atoms directly bonded to Si atoms are mainly retained in the glass structure.[42] Accordingly, the chemical analysis results, reported in Table II, show a very similar carbon content for the two M and MA25 Si–O–C samples, independently of the carbon content of the starting gel.

Both samples are thermally stable up to 1400°C, which is the onset temperature of the carbothermal reduction reactions. According to the thermogravimetric behavior, thermal treatments at 1000°C and 1300°C for 1 h holding time were performed on M and MA25 particles, and the FE-SEM study (Fig. 4) confirmed that even at 1300°C, the particles retain the spherical shape. An attempt to estimate the linear shrinkage of the particles during pyrolysis has been made by comparing the average diameter before and after the thermal

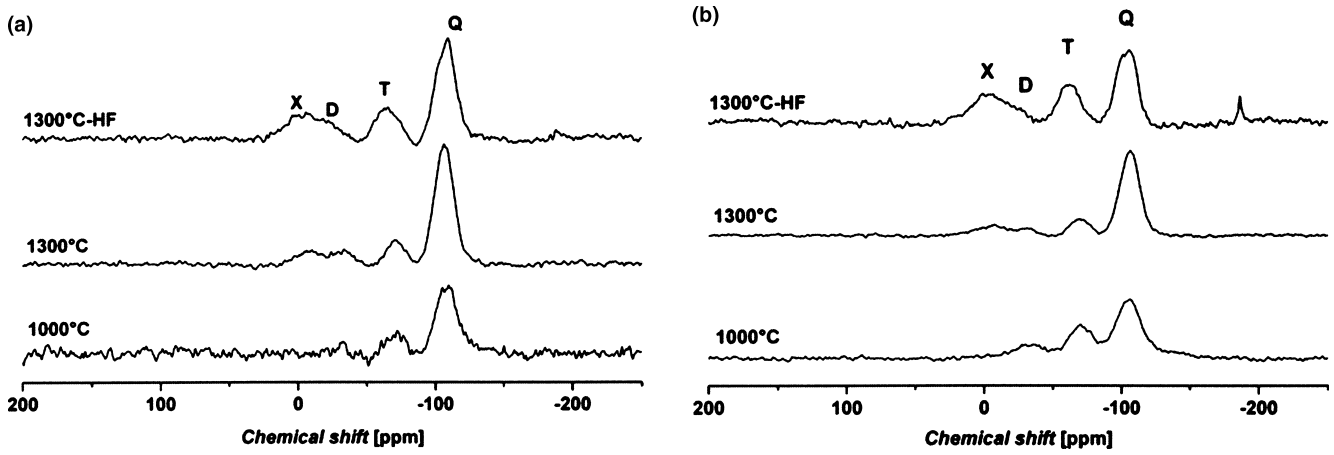

Fig. 5. (a) ^{29}Si SP MAS NMR spectra of M samples pyrolyzed for 1 h at 1000°C, 1300°C, and at 1300°C and subsequently HF etched; (b) ^{29}Si SP MAS NMR spectra of MA25 samples pyrolyzed for 1 h at 1000°C, 1300°C, and at 1300°C and subsequently HF etched.

Table III. Results of Quantitative Analysis from ^{29}Si SP MAS NMR Spectra of M and MA25 Nanoparticles Pyrolyzed at 1000°C, 1300°C for 1 h and after HF Etching

	Sample M				Sample MA25			
	Si units (%)				Si units (%)			
Pyrolysis temperature (°C)	X	D	T	Q	X	D	T	Q
1000	–	3.6	16,7	79,7	–	16,7	32,0	51,4
1300	10,2	7,5	12,4	70,0	12,9	5,9	13,1	68,0
1300 + HF etching	23,3	4,1	20,1	52,5	29.7	2,7	23,2	44,3

treatment. However, the large particle sizes dispersion, which is comparable or higher than the usual linear shrinkage reported in the literature for Si–O–C glasses (15%–20%),[43] leads to meaningless results.

The pyrolyzed nanoparticles are amorphous up to the maximum pyrolysis temperature, with XRD patterns featuring a main halo at 22° and a very weak and broad signal at around 35°, which are consistent with the presence of an amorphous oxycarbide phase.[30]

However, ^{29}Si MAS NMR is the best tool to assess the formation of the Si–O–C phase. Figure 5 shows the ^{29}Si SP MAS NMR spectra of M [Fig. 5(a)] and MA25 [Fig. 5(b)] samples after pyrolysis at 1000°C and 1300°C for 1 h. Peaks due to X (SiC_4), D (SiC_2O_2) T ($SiCO_3$) and Q (SiO_4) silicon units, at around −10, −35, −70, and −110 ppm, respectively, are present in the spectra and represent the fingerprints of the silicon oxycarbide network.[44] The spectra have been simulated and the results of the quantitative analysis are reported in Table III. Increasing the pyrolysis temperature from 1000°C to 1300°C leads to the formation of SiC_4 sites.

The microstructural features (specific surface area SSA, pore size distribution PSD, and total pore volume TPV) were investigated by N_2 adsorption analysis and the results are reported in Table IV. M and MA25 hybrid submicrometer-sized particles are characterized by a high-condensation degree[34] and the N_2 sorption analysis highlights a low porosity at the xerogel state, with small SSA and TPV values due to the presence of few micropores (Table IV). The BET SSA measured after pyrolysis at 1000°C is around 20 m^2/g for both samples, but the TPV value of MA25 increases due to the formation of few large pores with diameter in the range 10–100 nm that are stable up to 1300°C. The measured surface area values can be attributed to the geometrical external surface of the particles, which can be calculated assuming the typical density of the Si–O–C phase[14] and diameters of 100–400 nm. The BET SSA and pore volume for the M sample pyrolyzed at 1300°C have not been measured; however, based on TGA results showing the thermal stability up to 1400°C and on our experience in this field,[31] we do not expect any important microstructural evolution for this sample at this temperature. These results indicate that in the as-pyrolyzed state, the Si–O–C particles are essentially dense and not porous.

(3) HF Etching of Silicon Oxycarbide Submicrometer-Sized Particles

With the aim of preparing highly porous silicon oxycarbide submicrometer-sized particles, M and MA25 samples, pyrolyzed at 1300°C, have been treated with aqueous HF. Indeed, several studies have shown that HF etching of SiCO and SiBCO preferentially dissolves the silica clusters leaving behind highly porous C-rich SiCOs.[30–33] The chemical etching does not affect the morphology of the oxycarbide particles, which retain their regular shape and do not show any tendency to increase the aggregation (Fig. 4). The NMR study [Fig. 5(a) and (b)] confirms the selective dissolution of the silica-rich phase, the amount of Q units being largely reduced in both samples, while the relative concentration of SiC_4 units increases (Table III). A sharp signal, accounting

Table IV. Nitrogen Sorption Data of M and MA25 Nanoparticles Pyrolyzed at 1000°C, 1300°C for 1 h and after HF Etching

	Sample M		Sample MA25	
Pyrolysis Temperature (°C)	BET SSA (m^2 g^{-1})	TPV (cm^3 g^{-1})	BET SSA (m^2 g^{-1})	TPV (cm^3 g^{-1})
25	47	0.06	27.0	0.06
1000	20	0.07	23	0.2
1300	–	–	22	0.2
1300 + HF etching	406	0.4	564	0.7

for <2%, is detected at −188 ppm and is tentatively attributed to the presence of residual fluorine-substituted species, entrapped into the network.

The selective removal of the silica phase generates highly porous nanoparticles (Table IV). The N_2 adsorption isotherms (Fig. 6) are typical of solids with micro and mesopores (Types I and II isotherms). The pore size distribution curves (Fig. 7), present the main component due to the micropores (visible starting from $d = 1.7$ nm) and a second component at around 2 nm in diameter. The consequence is the net increase in both the TPV and SSA: the total pore volume reaches values of 0.4 and 0.7 cc/g, and the SSA reaches values of 406 and 564 m^2/g for M and MA25, respectively (see Table IV). We believe that these Si–O–C nanoparticles could have a broad spectrum of possible applications. Work to assess the behavior of the Si–O–C submicrometer-sized particles as anode for Li-ion batteries is currently under investigation.

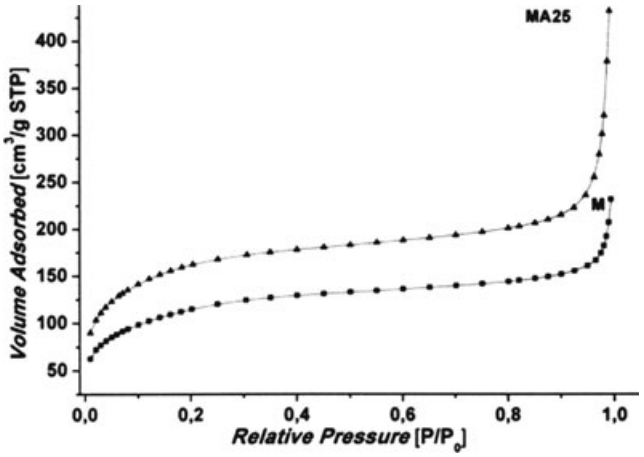

Fig. 6. Nitrogen adsorption isotherms of M and MA25 samples heated at 1300°C for 1 h and subsequently HF etched.

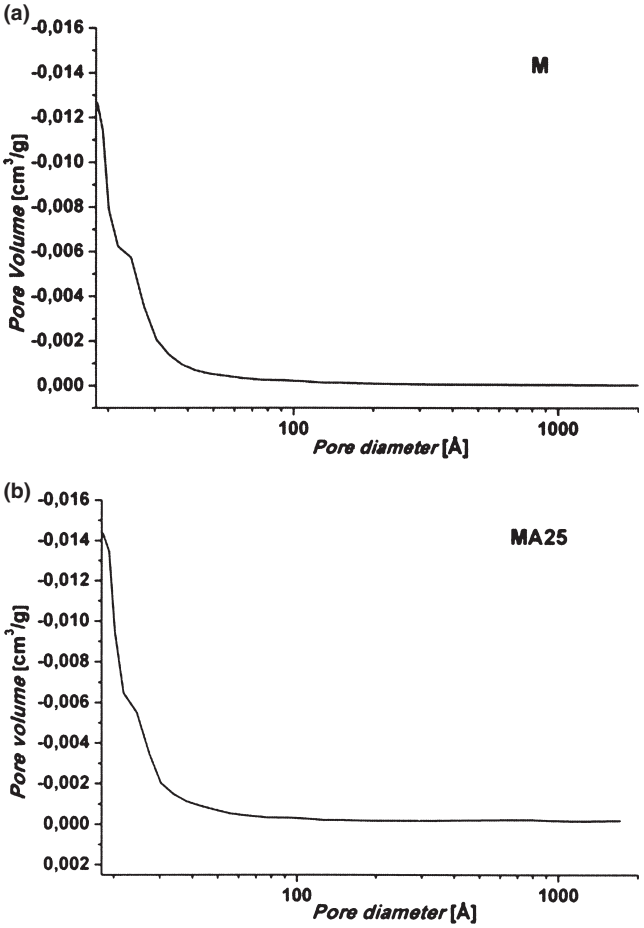

Fig. 7. Pore size distribution obtained from N_2 adsorption isotherms of M (a) and MA25 (b) samples heated at 1300°C for 1 h and subsequently HF etched.

IV. Conclusions

We have shown that the polymer pyrolysis route in conjunction with a modified Stöber process allows preparing Si–O–C spheres with diameter in the range 100–400 nm. Among the various compositions studied, the ability of retaining the spherical shape after pyrolysis was demonstrated in the case of particles prepared from pure MTES and 75/25 mol% MTES/ATES. For spheres prepared from pure phenyltrieth-oxysilane or mixed MTES/ATES with an ATES content higher than 25 mol%, the glass transition temperature of the silsesquioxane network is lower than the onset of the polymer-to-ceramic transformation preventing the shape retention during pyrolysis.

The dense Si–O–C particles obtained after pyrolysis can be further converted into highly porous submicrometer-sized spheres by HF etching the silica nanodomains of the silicon oxycarbide network. Accordingly, SSA up to 564 m^2/g and pore volume up to 0.7 cm^3/g can be obtained.

Acknowledgments

S. Dirè wishes to acknowledge the financial support of MIUR (PRIN 2007). G. D. Sorarù wishes to acknowledge the financial support of the EU through the contract MC-RTN-019601, PolyCerNet. The authors acknowledge BIO-tech (University of Trento) for FE-SEM analyses. Dr. E. Callone (University of Trento) is gratefully acknowledged for the NMR measurements. Dipl.-Ing. Cludia Fasel (Technische Universität Darmstadt) is gratefully acknowledged for the chemical analysis.

References

[1]P. Colombo, G. Mera, R. Riedel, and D. D. Soraru, "Polymer-Derived Ceramics: 40 Years of Research and Innovation in Advanced Ceramics," *J. Am. Ceram. Soc.*, **93**, 1805–37 (2010).

[2]R. Riedel, A. Kienzle, W. Dressler, L. Ruwisch, J. Bill, and F. Aldinger, "A Silicoboron Carbonitride Ceramic Stable to 2,000°C," *Nature*, **382**, 796–8 (1996).

[3]R. Riedel, L. M. Ruswisch, L. An, and R. Raj, "Amorphous Silicoboron Carbonitride Ceramic with Very High Viscosity at Temperatures above 1500°C," *J. Am. Ceram. Soc.*, **81**, 3341–4 (1998).

[4]S. Yajima, J. Hayashi, and M. Imori, "Continuous Silicon Carbide Fiber of High Tensile Strength," *Chem. Lett.*, 931–4 (1975).

[5]T. Ishikawa, Y. Kohtoku, K. Kumagawa, T. Yamamura, and T. Nasagawa, "High-Strenght, Alkali-Resistant Sintered SiC Fibre Stable up to 2,200°C," *Nature*, **391**, 773–5 (1998).

[6]L. V. Interrante, C. W. Whitmarsh, and W. J. Sherwood, "Fabrication of SiC Matrix Composites Using a Liquid Polycarbosilane as the Matrix Source," *Ceram. Trans.*, **58**, 111–5 (1995).

[7]P. Colombo, V. Sglavo, E. Pippel, and J. Woltersdorf, "Joining of Reaction-Bonded Silicon Carbide Using a Preceramic Polymer," *J. Mater. Sci.*, **33**, 2409–16 (1998).

[8]A. Karakuscu, R. Guider, L. Pavesi, and G. D. Sorarù, "White Luminescence From sol-gel Derived SiOC Thin Films," *J. Am. Ceram. Soc.*, **92**, 2969–74 (2009).

[9]L. G. Zhang, Y. S. Wang, Y. Wei, W. X. Xu, D. J. Fang, L. Zhai, K. C. Lin, and L. An, "A Silicon Carbonitride Ceramic with Anomalously High Piezoresistivity," *J. Am. Ceram. Soc.*, **91**, 1346–439 (2008).

[10]H. Fukui, H. Ohsuka, T. Ohsuka, T. Hino, and K. Kanamura, "A Si-O-C Composite Anode: High Capability and Proposed Mechanism of Lithium Storage Associated with Microstructural Characteristics," *Appl. Mater. Interfaces*, **2**, 998–1008 (2010).

[11]A. Saha, R. Raj, and D. L. Williamson, "A Model for the Nanodomains in Polymer-Derived SiCO," *J. Am. Ceram. Soc.*, **89**, 2188–95 (2006).

[12]G. Mera, A. Tamayo, H. Nguyen, S. Sen, and R. Riedel, "Nanodomain Structure of Carbon-Rich SiCN Polymer-Derived Ceramics," *J. Am. Ceram. Soc.*, **93**, 1169–75 (2010).

[13]P. Greil, "Active-Filler-Controlled Pyrolysis of Preceramic Polymers," *J. Am. Ceram. Soc.*, **78**, 835–48 (1995).

[14]S. Walter, G. D. Sorarù, H. Brequel, and S. Enzo, "Microstructural and Mechanical Characterization of Sol Gel-Derived SiOC Glasses," *J. Eur. Ceram. Soc.*, **22**, 2389–400 (2002).

[15]H. Freimuth, V. Hessel, H. Kolle, M. Lacher, W. Erhfeld, T. Vaahs, and M. Bruck, "Formation of Complex Ceramic Miniaturized Structures by Pyrolysis of Poly(Vinylsilazane)," *J. Am. Ceram. Soc.*, **79**, 1457–65 (1996).
[16]L. A. Liew, W. G. Zhang, L. An, S. Shah, R. L. Luo, Y. P. Liu, T. Cross, M. L. Dunn, V. M. Bright, J. W. Daily, R. Raj, and K. Anseth, "Ceramic MEMS – New Materials, Innovative Processing and Futuristic Applications," *Am. Ceram. Soc. Bull.*, **80**, 25–30 (2001).
[17]C. Guizard, A. Bac, M. Barboiu, and N. Hovnanian, "Hybrid Organic-Inorganic Membranes With Specific Transport. Properties Applications in Separation and Sensors Technologies," *Sep. Purif. Technol.*, **25**, 167–80 (2001).
[18]S. C. Tjong, "Novel Nanoparticle-Reinforced Metal Matrix Composites With Enhanced Mechanical Properties," *Adv. Eng. Mater.*, **9**, 639–52 (2007).
[19]Y. Jin, A. Li, S. G. Hazelton, S. Liang, C. L. John, P. D. Selid, D. T. Pierce, and J. X. Zhao, "Amorphous Silica Nanohybrids: Synthesis, Properties and Applications," *Coord. Chem. Rev.*, **253**, 2998–3014 (2009).
[20]T. Mishra, J. Hait, N. Aman, M. Gunjan, B. Mahato, and R. K. Jana, "Surfactant Mediated Synthesis of Spherical Binary Oxides Photocatalytic With Enhanced Activity in Visible Light," *J. Colloid and Interf. Sci.*, **327**, 377–83 (2008).
[21]C. Feldmann, "Polyol Mediated Synthesis of Oxide Particle Suspensions and their Application," *Scr. Mater.*, **44**, 2193–6 (2001).
[22]M. Xu, Y.-N. Lu, Y.-F. Liu, S.-Z. Shi, T.-S. Qian, and D.-Y. Lu, "Sonochemical Synthesis of Monosized Spherical $BaTiO_3$ Particles," *Powder Technol.*, **161**, 185–9 (2006).
[23]W. Stöber, A. Fink, and E. Bohn, "Controlled Growth of Monodispersed Silica Spheres in the Micron Size Range," *J. Colloid Interface Sci.*, **26**, 62–9 (1968).
[24]S. Ishihara, T. Nishimura, and H. Tanaka, "Precipitation Processing to Synthesize Fine Polycarbosilane Particles for Precursors of Silicon Carbide Powders," *J. Ceram. Soc. Japan*, **114**, 507–10 (2006).
[25]V. Bakumov, M. Schwarz, and E. Kroke, "Emulsion Processing of Polymer-Derived Porous Si/C/(O) Ceramic Bodies," *J. Eur. Ceram. Soc.*, **29**, 2857–65 (2009).
[26]F. J. Suarez, M. Sevilla, S. Alvarez, T. Valdes-Solis, and A. B. Fuertes, "Synthesis of Highly Uniform Mesoporous Sub-Micrometric Capsules of Silicon Oxycarbide and Silica," *Chem. Mater.*, **19**, 3096–8 (2007).
[27]X. Yu, S. Ding, Z. Meng, L. Liu, X. Qu, Y. Lu, and Z. Yang, "Aerosol Assisted Synthesis of Silica/Phenolic Resin Composite Mesoporous Hollow Spheres," *Coll. Polym. Sci.*, **286**, 1361–8 (2008).
[28]J. Cordelair and P. Greil, "Electrical Conductivity Measurements as a Microprobe for Structure Transitions in Polysiloxane Derived Si–O–C Ceramics," *J. Eur. Ceram. Soc.*, **20**, 1947–57 (2000).
[29]R. Riedel, L. Toma, E. Janssen, J. Nuffer, T. Melz, and H. Hanselka, "Piezoresistive Effect in SiOC Ceramics for Integrated Pressure Sensors," *J. Am. Ceram. Soc.*, **93**, 920–4 (2010).
[30]A. M. Wilson, G. Zank, K. Eguchi, W. Xing, B. Yates, and J. R. Dahn, "Pore Creation in Silicon Oxycarbides by Rinsing in Dilute Hydrofluoric Acid," *Chem. Mater.*, **9**, 2139–44 (1997).
[31]R. Peña-Alonso, R. Raj, and G. D. Soraru, "Preparation of Ultrathin Walled Carbon Based Structures by Etching Pseudo-Amorphous Silicon-Oxycarbide Ceramics," *J. Am. Ceram. Soc.*, **89**, 2473–80 (2006).
[32]R. Pena-Alonso, G. Mariotto, C. Gervais, F. Babonneau, and G. D. Soraru, "New Insights on the High-Temperature Nanostructure Evolution of SiCO and B-Doped SiBOC Polymer-Derived Glasses," *Chem. Mater.*, **19**, 5694–702 (2007).
[33]P. Dibandjo, S. Dirè, F. Babonneau, and G. D. Soraru, "New Insights Into the Nanostructure of High-C SiCO Glasses Obtained via Polymer Pyrolysis," *Glass Tech. Eur. J. Glass Sci. Technol. A*, **49**, 175–8 (2008).
[34]S. Dirè, V. Tagliazucca, E. Callone, and A. Quaranta, "Effect of Functional Groups on Condensation and Properties of sol-gel Silica Nanoparticles Prepared by Direct Synthesis From Organoalkoxysilanes," *Mater. Chem. Phys.*, **126**, 909–17 (2011).
[35]M. D. Abramoff, P. J. Magelhaes, and S. J. Ram, "Image Processing With ImageJ," *Biophotonics Int.*, **11**, 36–66 (2004).
[36]M. Fedel, F. Deflorian, S. Dirè, V. Tagliazucca, R. Bongiovanni, and L. Vescovo, "Characterization of Nano-Structured UV Cured Acrylic Coatings," *ECS Trans.*, **24**, 51–66 (2010).
[37]S. Modena, G. D. Soraru, Y. Blum, and R. Raj, "Passive Oxidation of an Effluent System: The Case of a Polymer Derived SiOC," *J. Am. Ceram. Soc.*, **88**, 339–45 (2005).
[38]A. Matsuda, T. Sasaki, T. Tanaka, M. Tatsumisago, and T. Minami, "Preparation of Copolymerized Phenylsilsesquioxane-Benzylsilsesquioxane Particles," *J. Sol-Gel. Sci. Technol.*, **23**, 247–52 (2002).
[39]G. Das, P. Bettotti, L. Ferraioli, R. Raj, G. Mariotto, L. Pavesi, and G. D. Soraru, "Study of the Pyrolysis Process of an Hybrid CH3SiO1.5 Gel into a SiCO Glass," *Vib. Spectrosc.*, **45**, 61–8 (2007).
[40]D. Bahloul-Hourlier, J. Latournerie, and P. Dempsey, "Reaction Pathways During the Thermal Conversion of Polysiloxane Precursors into Oxycarbide Ceramics," *J. Europ. Ceram. Soc.*, **25**, 979–85 (2005).
[41]P. H. Mutin, "Control of the Composition and Structure of Silicon Oxycarbide and Oxynitride Glasses Derived from Polysiloxane Precursors," *J. Sol-Gel. Sci. Technol.*, **14**, 27–38 (1999).
[42]H. Zhang and C. G. Pantano, "Synthesis and Characterization of Silicon Oxycarbide Glasses," *J. Am. Ceram. Soc.*, **73**, 958–63 (1990).
[43]G. D. Sorarù, G. D'Andrea, R. Campostrini, and F. Babonneau, "Characterization of Methyl-Substituted Silica Gels with Si-H Functionalities," *J. Mater. Chem.*, **5**, 1363–74 (1995).
[44]H. Bréquel, J. Parmentier, S. Walter, R. Badheka, G. Trimmel, S. Masse, J. Latournerie, P. Dempsey, C. Turquat, A. Desmartin-Chomel, L. Le Neindre-Prum, U. A. Jayasooriya, D. Hourlier, H.-J. Kleebe, G. D. Sorarù, S. Enzo, and F. Babonneau, "Systematic Structural Characterisation of the High Temperature Behaviour of Nearly-Stoichiometric Silicon Oxycarbide Glasses," *Chem. Mater.*, **16**, 2585–98 (2004). □